Research Square

Preprints are preliminary reports that have not undergone peer review.
They should not be considered conclusive, used to inform clinical practice,
or referenced by the media as validated information.

Green synthesis of silver nanoparticles loaded in bacterial cellulose obtained from mothers of vinegar: In situ photoreduction, characterization, and antibacterial activity

Ana Beatriz Morales Cepeda

ana.mc@cdmadero.tecnm.mx

Instituto Tecnológico de Ciudad Madero

Abigail María Díaz-Guerrero

Instituto Tecnológico de Ciudad Madero

Karla Sintia Gallardo Urguell

Instituto Tecnológico de Ciudad Madero

Antonio Serguei Ledezma Pérez

Centro en Quimica Aplicada

Carmen Natividad Alvarado Canché

Centro en Quimica Aplicada

Jose Luis Rivera Armenta

Instituto Tecnológico de Ciudad Madero

Claudia Esmeralda Ramos Galvan

Instituto Tecnológico de Ciudad Madero

Claudia Alicia Castillo Miranda

Instituto Tecnológico de Ciudad Madero

Research Article

Keywords:

Posted Date: March 11th, 2026

DOI: https://doi.org/10.21203/rs.3.rs-8882830/v1

License: This work is licensed under a Creative Commons Attribution 4.0 International License.
Read Full License

Additional Declarations: No competing interests reported.

Green synthesis of silver nanoparticles loaded in bacterial cellulose obtained from mothers of vinegar: *In situ* photoreduction, characterization, and antibacterial activity

Ana Beatriz Morales-Cepeda[1,*], Abigail María Díaz-Guerrero[1*], Sintia Karla Gallardo-Urguell[1], Antonio Serguei Ledezma-Pérez[2], Carmen Natividad Alvarado-Canché[2], José Luis Rivera-Armenta[1], Claudia Esmeralda Ramos-Galván[3], Claudia Alicia Castillo-Miranda[3]

[1]Centro de Investigación en Petroquímica, Tecnológico Nacional de México/Instituto Tecnológico de Ciudad Madero, Parque Industrial Tecnia, Bahía de Aldahir S/N, 89603 Altamira, Tamaulipas, Mexico

[2]Departamento de Materiales Avanzados, Centro de Investigación en Química Aplicada, Blvd. Enrique Reyna H. 140, San José de los Cerritos, 25294 Saltillo, Coahuila, México

[3]Instituto Tecnológico de Ciudad Madero/Tecnológico Nacional de México, Av. Primero de Mayo s/N col. Los Mangos, Cd. Madero Tamaulipas, México

***Corresponding author**

E-mail: ana.mc@cdmadero.tecnm.mx; abigail.dg@cdmadero.tecnm.mx

Abstract

Silver nanoparticles (AgNPs) are known for their outstanding antimicrobial activity. However, most traditional methods used to synthesize silver nanoparticles require either the use of chemical reducing agents and activators that are highly polluting or that require investments in expensive equipment with high energy consumption. Thus, finding green, fast, and simple alternatives to synthesize silver particles for antiseptic purposes is important. In this study, AgNPs were synthesized *in situ* on a matrix of bacterial cellulose (BC) obtained from mothers of pineapple vinegar by a photoreduction reaction assisted by a sodium lamp that emitted yellow light (λ = 589 nm). BC-AgNP films were synthesized with AgNP concentrations of 5, 25, 50, 75, and 100 ppm, and their antibacterial activity was evaluated; the results revealed that they inhibited the growth of *Staphylococcus aureus* and *Escherichia coli* by up to 100% and 95.6%, respectively.

Introduction

Throughout history, silver and silver compounds have been widely used as antiseptics because of their extraordinary antimicrobial properties. Silver can inhibit the growth of several varieties of bacteria [1-3], fungi [4-6], and viruses [7-9] owing to a mechanism that deactivates the respiratory enzymes of cells [10, 11]. At present, researchers in the biomedical and pharmaceutical fields are especially interested in the use of silver nanoparticles (AgNPs) as alternatives to antibiotics, given that many of the most common pathogens are becoming resistant to an increasing number of drugs [12, 13]. However, most traditional methods used to synthesize AgNPs require the use of chemical reagents such as sodium borohydride, sodium citrate, and ethylene glycol, which are pollutants and can be dangerous to human health [14, 15]. Alternative methods, such as laser ablation, are expensive because of the equipment and energy they require to operate [16]. For these reasons, finding environmentally friendly (or "green") synthesis alternatives for obtaining silver nanoparticles is important.

In recent years, methods for the photochemical synthesis of metal nanoparticles have been widely studied because of their relative simplicity, versatility, and low negative impact on the environment [17, 18]. This type of synthesis method, also known as photoreduction, consists of reducing metal ions by irradiating them with either ultraviolet or visible light [19], as shown in Fig, 1. This method can be performed *in situ*, that is, directly on the matrix material that will be used to support the metal nanoparticles. Silver nanoparticles can be obtained from different precursor solutions by photoreduction reactions, and no other reducing agent is needed for the reaction to occur [20-22], although an acidic environment is often preferred.

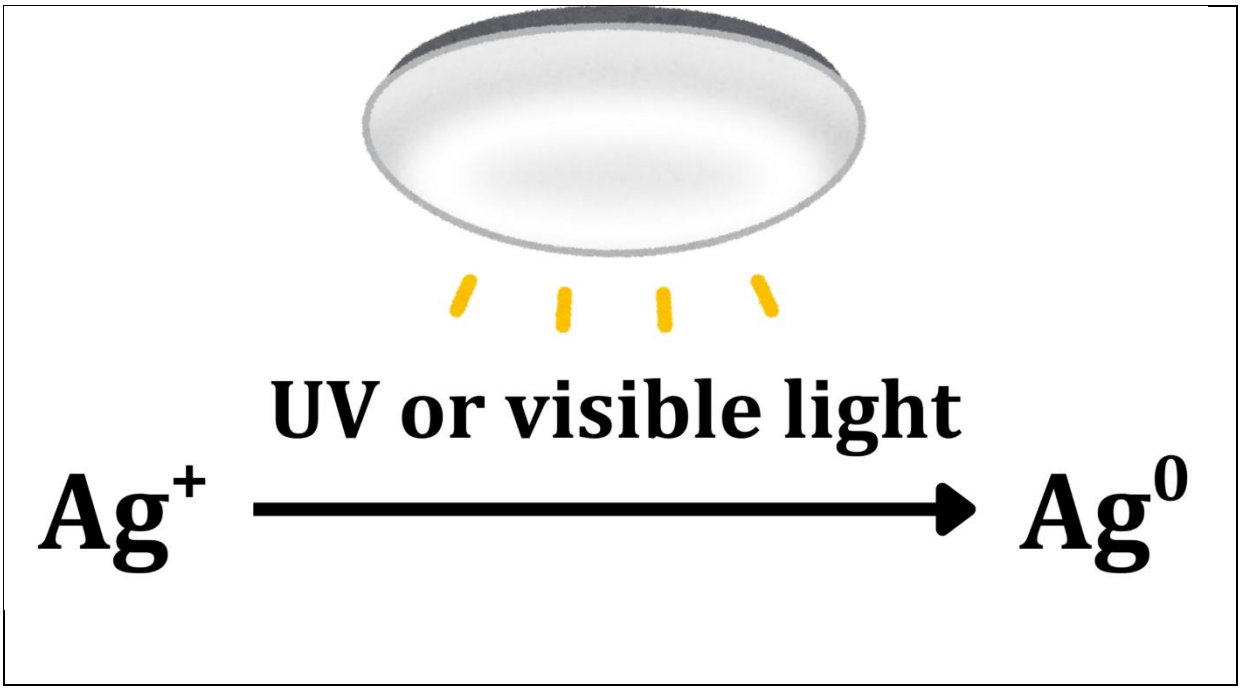


Fig. 1 Silver photoreduction

AgNPs are successfully photosynthesized on liquid matrices such as extracts of prickly pear and a mixture of lemon juice and commercial rice vinegar [23, 24], as well as in solid cellulose matrices with the aid of a natural green tree substrate as a reducing agent [25]. Bacterial cellulose, in particular, is a highly porous, biodegradable, and biocompatible material that is easy to functionalize and has great mechanical strength and low density, which makes it an ideal material for use as a support for drugs and metal nanoparticles with healing purposes [26-28]. Silver particles that are directly photosynthesized on a cellulose matrix are deposited onto the gel network and chemically bonded to the surfaces of the fibers [29], and reports have demonstrated that BC-AgNP films present outstanding antibacterial activity [29, 30]. However, there are no reports of AgNPs being photosynthesized *in situ* on bacterial cellulose matrices obtained from mothers of vinegar, even though mothers of vinegar are a source of highly pure bacterial cellulose (BC), which has the advantage of not being mixed with

hemicellulose, pectin, and lignin, as is often the case for cellulose obtained from plants [31].

In this study, silver nanoparticles were photosynthesized from a silver nitrate precursor and directly deposited onto a bacterial cellulose matrix to produce antimicrobial films with potential use as topical antiseptics. The photoreduction reaction was carried out using a sodium lamp emitting yellow light (λ = 589 nm) and was performed in an ultrasound bath to guarantee the correct dispersion of the metal particles in the matrix. The BC used in this research was obtained from mothers of pineapple vinegar. The BC-AgNP films were synthesized at AgNP concentrations of 5, 25, 50, 75, and 100 ppm and characterized by optical microscopy, Fourier transform infrared spectroscopy (FTIR), thermogravimetric analysis (TGA), and scanning electron microscopy (SEM). The antibacterial activity of the films was evaluated against *Staphylococcus aureus* and *Escherichia coli*, which are the two most common sources of bacterial infections in hospitals and health care facilities worldwide [32, 33] and have been reported to present significant and constantly increasing antimicrobial resistance (MRA) against multiple antibiotics, such as penicillins, cephems, fluoroquinolones, and tetracyclines [34-36]. The results showed that the BC-AgNP films can inhibit the growth of *S. aureus* and *E. coli* by up to 100% and 95.6%, respectively.

Materials and methods

Bacterial cellulose was obtained from mothers of vinegar, specifically pineapple vinegar. The mothers of vinegar were subsequently washed two or three times in isopropyl alcohol and then with distilled water until they reached a pH between 4 and 5.

All the washing was performed at room temperature under stirring. The obtained cellulose was crushed and separated into samples of approximately five grams each. The samples were poured into glass vials and soaked with the silver nitrate solution at the corresponding concentrations to obtain films with 5, 25, 50, 75, or 100 ppm of silver nanoparticles. The vials containing the samples were perfectly sealed and placed in an ultrasonic bath under the light of a sodium lamp for 1 hr. The samples were then poured into trays with areas of 2.5 × 2.5 cm, rinsed with distilled water to remove impurities, and left to dry for two to three weeks until solid films were formed. Control samples of pure BC without silver were subjected to the same procedure.

The obtained films were characterized via optical microscopy, Fourier transform infrared spectroscopy (FTIR), thermogravimetric analysis (TGA), and scanning electron microscopy (SEM). Optical micrographs were obtained by a ZEISS AX10 microscope (Germany) and visualized with Motic Images Plus software (version 3.0). FTIR analysis was carried out with a PerkinElmer Spectrum 100 spectrophotometer (Shelton, CT, USA) in the range of 4000–700 cm^{-1}. TGA was performed with a TA SDT Q600 thermogravimetric analyzer (New Castle, Delaware, USA) at temperatures between 0 and 600 °C with a heating rate of 10 °C min^{-1} under a N_2 atmosphere. Finally, SEM micrographs were obtained with a JEOL JSM IT200 system (Zurich, Switzerland) using a sample size of approximately 20 mm^2.

The antibacterial activity of the films was tested against *Escherichia coli* ATCC-25922 and *Staphylococcus aureus* ATCC-29213 using the Japan Industrial Standard JIS Z 2801:2000 method (Japanese Standards Association 2000) with minor modifications, as described by Morales-Cepeda et al. [37] Each bacterium was

individually grown in trypticase soy broth (TSB), and these cultures were used to prepare suspensions in a solution of NaCl (0.85%). Inoculum concentrations were calculated using the viable plate count method. The number of colony-forming units per milliliter (CFU mL^{-1}) was adjusted to approximately 51,000 with trypticase soy broth (1/500). The sample films were placed into sterile vials, inoculated with 4 mL of this suspension, and incubated at 37 °C for 24 h in a humidified atmosphere (90%). After incubation, the number of CFUs was calculated through plate counting on trypticase soy agar (TSA), and the antibacterial activity (R) values were obtained using the following equation:

$$R = Log\frac{control_{24h}}{control_{0h}} - Log\frac{sample_{24h}}{control_{0h}} \quad (1)$$

where $control_{24h}$ and $control_{0h}$ are the mean numbers of colonies in the vial without sample film at 24 h and 0 h, respectively, and $sample_{24h}$ is the mean number of bacteria in the sample film at 24 h. Finally, the growth inhibition percentage was calculated as follows:

$$Inhibition(\%) = \frac{CFU_{control} - CFU_{sample}}{CFU_{control}} * 100 \quad (2)$$

where $CFU_{control}$ and CFU_{sample} are the numbers of colonies in the vial without film and with the film sample, respectively. All tests were conducted in triplicate, and the average values are reported.

Results and discussion

After the mothers of vinegar were washed, bacterial cellulose was obtained in the form of transparent, whitish wet layers. After the photoreduction reaction, the sample

color changed from white to gray, as expected according to Pal et al. [29] and A. A. H. Abdellatif et al. [38] Dry films of BC-AgNPs and pure BC are shown in Fig. 2.



Fig. 2 BC-AgNP (left) and pure BC (right) films after drying

Characterization of the samples

Optical microscopy

Pure BC and BC-AgNP films were observed with an optical microscope at 10× with a 75° prism opening, and polarized mode was used to detect the silver metallic particles. The optical micrographs of pure BC and 25, 50, and 100 ppm BC-AgNP films are shown in Fig. 3. Although the diameter of any individual nanoparticle could not be detected or determined at 10× magnification, some clusters formed by aggregated particles can be observed in the micrographs. The micrographs of the loaded films

indicated that the silver nanoparticles formed clusters with lengths of approximately 100–135 µm at concentrations of 25 ppm, 125–250 µm at 50 ppm, and 180–450 µm at 100 ppm. These clusters formed because of the large specific area of the silver nanoparticles, which increases their thermodynamic attraction to each other and their tendency to aggregate [39, 40].

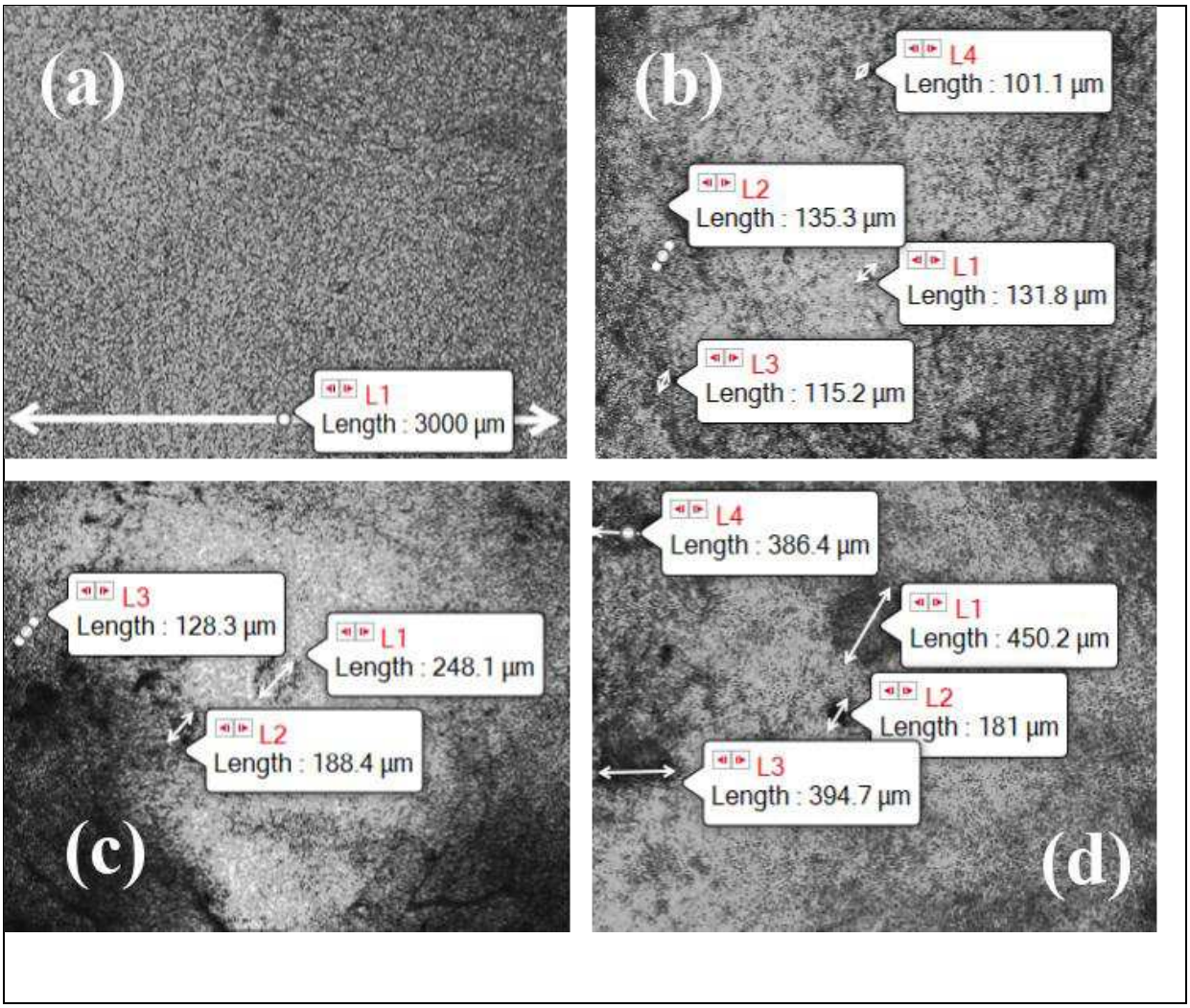


Fig. 3 Optical micrographs of (a) pure BC and BC-AgNPs at AgNP concentrations of (b) 25, (c) 50, and (d) 100 ppm

Fourier transform infrared spectroscopy (FTIR)

The FTIR spectra of the pure BC and BC-AgNP films are shown in Fig. 4. The intensity of the O–H absorption band at 3292.62 cm^{-1} decreases slightly with increasing silver concentration, which suggests that oxygen could have reacted with silver to form secondary compounds, leading to a decrease in the number of O–H bonds [41, 42]. However, the peaks corresponding to C–H stretching at 2932.82 cm^{-1} showed no variation depending on the amount of silver present in the sample, which indicates that the longer chains in the polymer were not affected by any chemical interaction occurring between carbon and silver [43]. N≡C stretching can be observed at 2115.11 cm^{-1} [44]. This peak was stronger with increasing amount of silver in the sample, which indicates that the nitrogen interacting with the carbon could be a remnant of the silver nitrate precursor. Finally, the peaks at 1640.24 cm^{-1} and 1104.89 cm^{-1}, corresponding to C=C and C–O stretching vibrations, respectively, remained constant regardless of the amount of silver in the sample [45, 46].

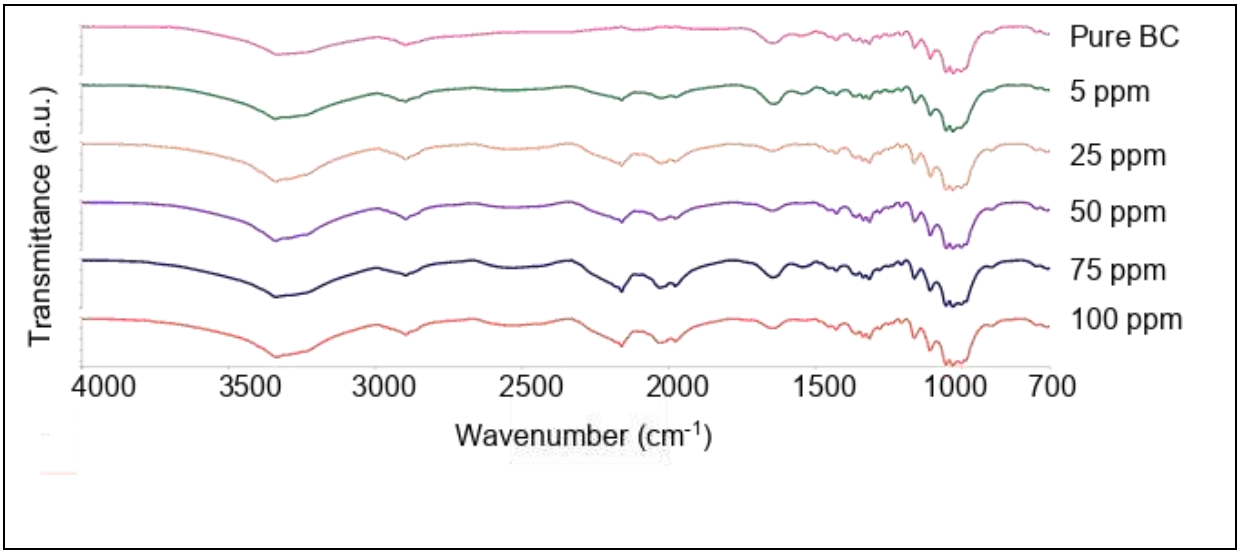


Fig. 4 FTIR spectra of pure BC and BC-AgNP films

Thermogravimetric analysis (TGA)

Thermogravimetric analysis (TGA) and derivative thermogravimetry (DTG) curves for the pure BC and BC-AgNP films are shown in Fig. 5. All the thermogravimetric analyses were carried out in the range of 0–600 °C. The first stage of mass loss for both samples, corresponding to a weight loss of ~5%, occurred between room temperature and approximately 100 °C, which can be attributed to the evaporation of water from the films [47, 48]. Afterward, the TGA curves remained stable up to approximately 250 °C, with a mass loss of ~2% in this region. The greatest mass loss occurred in the region between 250 and 360 °C, with losses of ~60% and ~55% for the pure BC sample and the BC-AgNP film, respectively. This large weight loss corresponds to the degradation of cellulose [49-51]. The last degradation stage, from 360 to 600 °C, corresponds to the loss of carbonaceous residues [52]. The mass remaining above 600 °C corresponds to the amount of ash in the pure BC samples and to the added weight of the ashes and silver nanoparticles in the BC-AgNP films. Compared with the pure cellulose samples, the films with silver retained approximately 2% more mass. The DTG curves indicated that the thermal degradation of the samples occurred mainly in the 260–380 °C region, with the maximum decomposition rates being at 345 and 350 °C for the pure BC and BC-AgNP films, respectively. Compared with pure BC, the BC-AgNP films presented a slightly lower degradation rate, as silver likely increased the thermal stability of the samples [50, 53].

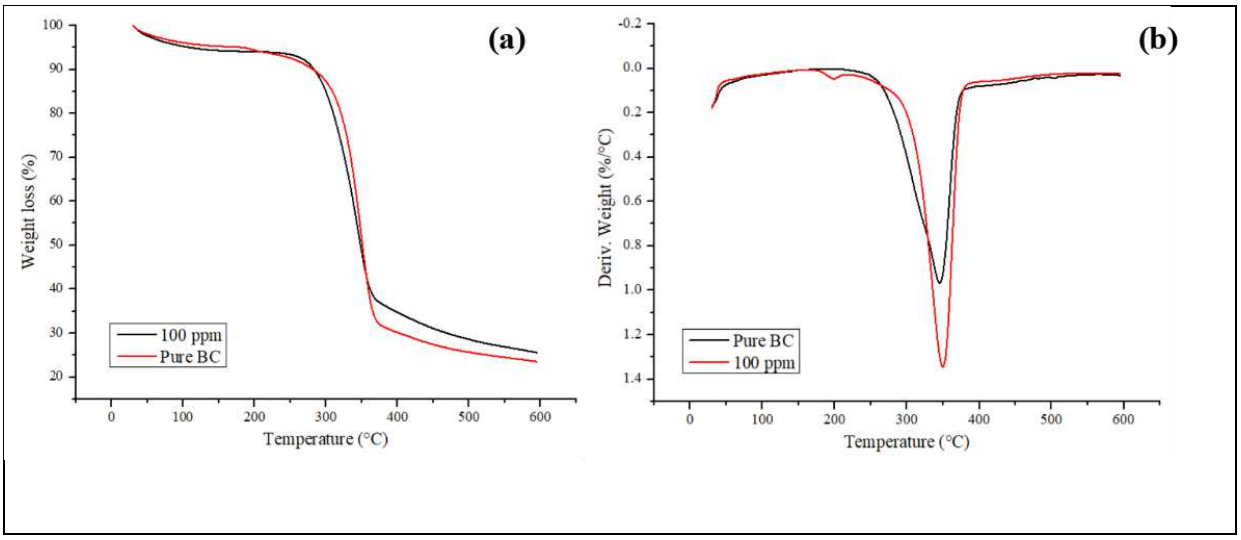


Fig. 5 Comparison of the (a) TGA and (b) DTG curves for BC and a BC-AgNP film at an AgNP concentration of 100 ppm

Scanning electron microscopy (SEM)

SEM micrographs of a BC-AgNP film with a concentration of 100 ppm are shown in Fig. 6. The micrographs were obtained at magnifications of 30× and 1400× (a) and at 100× and 3500× (b). The silver particles that formed in the bacterial cellulose matrix tended to be either spherical or oval-like semispheres, and appeared to be highly agglomerating given their rough surface. In both images, microparticles with sizes between 10 and 20 μm can be observed, as can nanoparticles with sizes between 10 and 100 nm, which are either scattered around the films or clustered on the surfaces of the larger microparticles. Larger microparticles likely formed because the reaction was performed in an environment with a pH between 4 and 4.5, as lower pH values favor the formation of larger particles [54]. However, the fact that most of the particles were spherical or semispherical indicates that the combination of yellow light and the vibrations of the ultrasonic bath is optimal, as controlling and unifying the shape of silver

nanoparticles can be difficult to achieve, particularly when alternative synthesis methods are used [55].

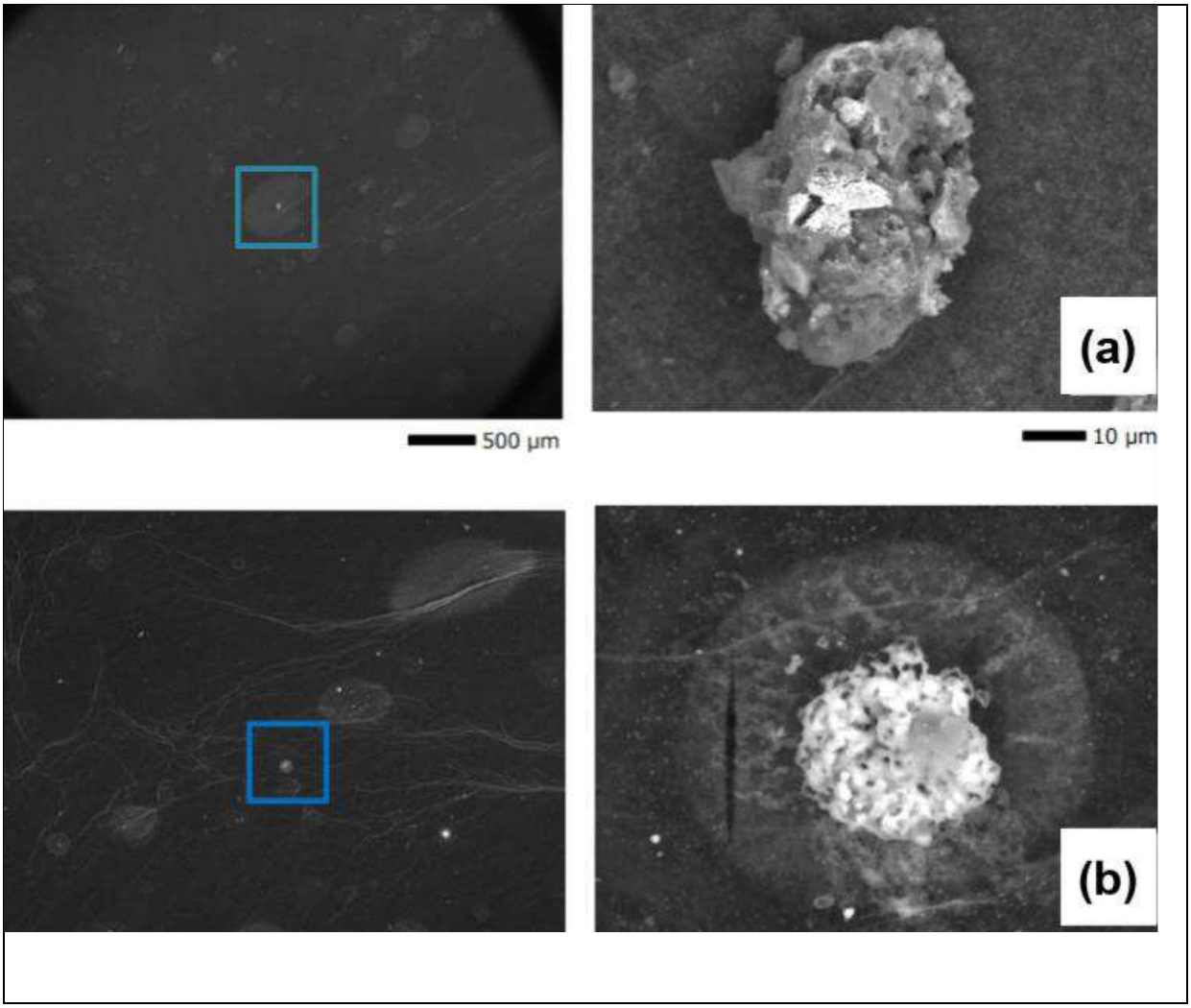


Fig. 6 SEM micrographs of a BC-AgNP film with (a) oval and (b) spherical particles

Antibacterial activity testing

Table 1 displays the antibacterial activity (R) values and the percentages of growth inhibition of the BC-AgNP films against *E. coli* and *S. aureus*. The pure BC films did not present significant antimicrobial activity against either of the bacteria; therefore, the bacterial cultures evaluated with these samples did not show any growth inhibition.

All the samples with silver nanoparticles, on the other hand, presented antibacterial activity with values equal to or greater than 2, which means that these materials are effective for antimicrobial use [56], with the potential to be used as topical antiseptics for the treatment of superficial wounds [57, 58]. However, the BC-AgNPs performed better against *S. aureus* than against *E. coli*, reaching maximum inhibition percentages of 100% and 95.6%, respectively. In addition, when tested against *S. aureus*, the films presented growth inhibition percentages above 90% at every concentration; however, when tested against *E. coli*, only the BC-AgNP films with silver concentrations equal to or greater than 50 ppm presented growth inhibition values above 90%. These findings are in line with previous research, where it has been reported that the same antimicrobial material can have different effects against different microorganisms [29, 59, 60]. Notably, compared with those of reported AgNPs synthesized by green methods, the antimicrobial activity and growth inhibition of the BC-AgNP films synthesized in this study were outstanding. Silver nanoparticles synthesized using *Brassica carinata* extract as a reducing agent achieved growth inhibition percentages of only 50% against both *S. aureus* and *E. coli* at a concentration of 125 μg/mL (125 ppm) [61]. When synthesized using *Murraya koenigii* extract, the growth inhibition of *S. aureus* was only 31.4%, 53.3%, and 85.6% at 8, 16, and 32 μg/ml (ppm), respectively, although the inhibition of *E. coli* was greater than 81% at concentrations as low as 16 μg/ml (ppm) [62]. However, the values of growth inhibition of the AgNPs synthesized using *Hellenia speciosa* as the reducing agent were similar to those reported in this study, with 92.41% growth inhibition against *S. aureus* at a concentration of 25 μg/ml (25 ppm) [63]. On the other hand, silver nanoparticles synthesized via photoreduction

assisted by a femtosecond laser inhibited the growth of *E. coli* by approximately 65% at concentrations of 0.0081 g in 100 mL of solution (81 ppm) and 100% at concentrations of 0.0137 g and 0.0239 g per 100 mL of water (137 and 239 ppm, respectively) [64]. Notably, BC-AgNP films synthesized via more traditional chemical methods have been reported to inhibit the growth of both *E. coli* and *S. aureus* by up to 99 and 100% [30, 37]; however, these methods have the disadvantage of depending on polluting chemical reagents.

Table 1. Values of antibacterial activity (R) and growth inhibition (%) for the pure BC and BC-AgNP films against *E. coli* and *S. aureus*

Bacteria and Silver concentration (ppm)	Total bacterial count T0[a] (UFC/mL)		Total bacterial count T24[a] (UFC/mL)		Value of antibacterial activity (R)	Growth inhibition (%)
	Repetitions	Mean (SD[b])	Repetitions	Mean (SD[b])		
Escherichia coli ATCC-25922	5.00E ± 04 5.00E ± 04 5.00E ± 04	5.00E ± 04 (0)				
Control			N.A.	1.70E ± 07 (N.A.)	N.A.	N.A.
0			5.91E ± 07 4.84E ± 07	5.38E ± 07 (7.57E ± 06)	0.5	N.A.
5			1.35E ± 04 9.15E ± 03 1.15E ± 04	1.13E ± 04 (2.18E ± 03)	3.17	77.2
25			1.17E ± 04 1.05E ± 04 1.70E ± 04	1.30E ± 04 (3.46E ± 03)	3.11	73.8
50			4.25E ± 03 5.00E ± 03 3.50E ± 03	4.25E ± 03 (7.50E ± 02)	3.60	91.5
75			2.75E ± 03 4.60E ± 03 3.00E ± 03	3.45E ± 03 (1.00E ± 03)	3.69	93.1
100			2.15E ± 03 2.41E ± 03 2.00E ± 03	2.18E ± 03 (2.07E ± 02)	3.88	95.6
Staphylococcus aureus ATCC-29213	5.00E ± 04 5.00E ± 04 5.00E ± 04	5.00E ± 04 (0)				
Control			9.40E ± 07 1.08E ± 08	9.75E ± 07 (9.90E ± 06)	N.A.	N.A.
0			5.40E ± 07	5.40E ± 07 (0)	0.26	0
5			3.0E ± 03 5.0E ± 02 1.2E ± 03	1.57E ± 03 (1.29E ± 03)	4.79	96.8

25	7.35E ± 03 6.00E ± 02 4.7E ± 03	4.22E ± 03 (3.40E ± 03)	4.36	91.5
50	2.15E ± 02 2.50E ± 02 1.00E ± 02	1.88E ± 02 (7.85E ± 01)	5.71	99.6
75	5.00E ± 02 3.00E ± 02 2.00E ± 02	3.33E ± 02 (1.53E ± 02)	5.46	99.3
100	0 0 0	0 (0)	> 5.71	100

Notes:

[a] T0 and T24 indicate the time (in hours) at which bacterial counting was performed.

[b] SD indicates the standard deviation of the group of samples.

Conclusions

In this work, silver micro- and nanoparticles were synthesized by a green photoreduction method assisted by a sodium lamp that emitted yellow light, with no other chemical reagents used in the reaction other than the silver nitrate precursor. The AgNPs were synthesized *in situ* on a bacterial cellulose layer obtained from mothers of pineapple vinegar, and the reaction was carried out in an ultrasound bath to improve the dispersion of the particles in the polymeric matrix. The resulting BC-AgNP films were characterized via optical microscopy, FTIR, TGA, and SEM, and the silver nitrate precursor was successfully reduced into silver micro- and nanoparticles with spherical and oval-like semispherical shapes. The antimicrobial effectiveness of the AgNP films was evaluated against *Escherichia coli* and *Staphylococcus aureus*. The growth of *E. coli* decreased by more than 90% when the concentration of silver was as low as 50 ppm, with this value reaching up to 95.6% when the concentration was 100 ppm. On the other hand, the growth of *S. aureus* was inhibited by more than 90% at silver concentrations as low as 5 ppm, reaching a total growth inhibition of 100% when the BC-AgNP film concentration was 100 ppm. These results prove that photoreduction synthesis assisted by a sodium lamp is a promising method for obtaining silver micro- and nanoparticles with remarkable antibacterial properties. However, the aim of the present study was limited to proving the feasibility of photosynthesizing AgNPs on a BC support obtained from mothers of vinegar by using the proposed method and verifying that the obtained films exhibit good antibacterial activity.

Acknowledgements

Abigail María Díaz-Guerrero was supported by a postdoctoral fellowship from Consejo Nacional de Humanidades, Ciencias y Tecnologías (CONAHCYT). Sintia Karla Gallardo-Urguell received support from Consejo Nacional de Humanidades, Ciencias y Tecnologías (CONAHCYT) to pursue her graduate studies in the academic program of Maestría en Ciencias en Ingeniería Química at Tecnológico Nacional de México/Instituto Tecnológico de Ciudad Madero. The authors would also like to thank the Tecnológico Nacional de México for the support received through the calls for Projects of Scientific Research, Technological Development and Innovation in 2024, 2025 and 2026. This research was developed at Tecnológico Nacional de México/Instituto Tecnológico de Ciudad Madero, and the antibacterial activity tests were performed at the Departamento de Materiales Avanzados from Centro de Investigación en Química Aplicada.

Funding

This research was funded by Consejo Nacional de Humanidades, Ciencias y Tecnologías (CONAHCYT), and Tecnológico Nacional de México through the calls for Projects of Scientific Research, Technological Development and Innovation in 2024, 2025 and 2026.

Ethics statement

Not applicable

Author contributions Conceptualization, Morales-Cepeda, A.B., Castillo-Miranda, C.A. and Ramos-Galván, C.E.; methodology, Díaz-Guerrero, A.M.; validation, Ledezma-Pérez, A.S. and Alvarado-Canché, C.N.; formal analysis, Gallardo-Urguell, S.K., Ledezma-Pérez, A.S. and Rivera-Armenta, J.L.; investigation, Gallardo-Urguell, S.K.; resources, Morales-Cepeda, A.B., Castillo-Miranda, C.A. and Ramos-Galván, C.E.; data curation, Gallardo-Urguell, S.K.; writing—original draft preparation, Díaz-Guerrero, A.M.; writing—review and editing, Díaz-Guerrero, A.M. and Morales-Cepeda, A.B.; visualization, Gallardo-Urguell, S.K., Morales-Cepeda, A.B. and Díaz-Guerrero, A.M.; supervision, Morales-Cepeda, A.B.; project administration, Morales-Cepeda, A.B.; funding acquisition, Morales-Cepeda, A.B., Castillo-Miranda, C.A. and Ramos-Galván, C.E. All authors have read and agreed to the published version of the manuscript

Competing interests

The authors have no conflicts of interest to declare.

Dual publication

Not applicable

Data availability

The authors declare that the data supporting the findings of this study are available within the paper. Should any raw data files be needed in another format they are available from the corresponding author upon reasonable request.

References

1. Logambal S, Thilagavathi T, Chandrasekar M, Inmozhi C, Kedi PBE, Bassyouni FA, et al. Synthesis and antimicrobial activity of silver nanoparticles: incorporated couroupita guianensis flower petal extract for biomedical applications. J King Saud Univ Sci. 2023;35(1):102455. https://doi.org/10.1016/j.jksus.2022.102455.
2. Hasnain MS, Javed MN, Alam MS, Rishishwar P, Rishishwar S, Ali S, et al. Purple heart plant leaves extract-mediated silver nanoparticle synthesis: optimization by Box-Behnken design. Mater Sci Eng C. 2019;99:1105–14. https://doi.org/10.1016/j.msec.2019.02.061.
3. Echavarría JO, Vanegas NAG, Orozco CPO. Chitosan/carboxymethyl cellulose wound dressings supplemented with biologically synthesized silver nanoparticles from the ligninolytic fungus Anamorphous *Bjerkandera* sp. R1. Heliyon. 2022;8(9):e10258. https://doi.org/10.1016/j.heliyon.2022.e10258.
4. Wen H, Shi H, Jiang N, Qiu J, Lin F, Kou Y. Antifungal mechanisms of silver nanoparticles on mycotoxin producing rice false smut fungus. iScience. 2023;26(1):105763. https://doi.org/10.1016/j.isci.2022.105763.
5. Shi H, Wen H, Xie S, Li Y, Chen Y, Liu Z, et al. Antifungal activity and mechanisms of AgNPs and their combination with azoxystrobin against *Magnaporthe oryzae*. Environ Sci Nano. 2023;10(9):2412–26. https://doi.org/10.1039/d3en00168g.
6. Hashem AH, Saied E, Amin BH, Alotibi FO, Al-Askar AA, Arishi AA, et al. Antifungal activity of biosynthesized silver nanoparticles (AgNPs) against

Aspergilli causing Aspergillosis: ultrastructure study. J Funct Biomater. 2022;13(4):242. https://doi.org/10.3390/jfb13040242.

7. Allawadhi P, Singh V, Khurana A, Khurana I, Allwadhi S, Kumar P, et al. Silver nanoparticle based multifunctional approach for combating COVID-19. Sens Int. 2021;2:100101. https://doi.org/10.1016/j.sintl.2021.100101.
8. Naumenko K, Zahorodnia S, Pop CV, Rizun N. Antiviral activity of silver nanoparticles against the influenza A virus. J Virus Erad. 2023;9(2):100330. https://doi.org/10.1016/j.jve.2023.100330.
9. Luceri A, Francese R, Lembo D, Ferraris M, Balagna C. Silver nanoparticles: review of antiviral properties, mechanism of action and applications. Microorganisms. 2023;11(3):629. https://doi.org/10.3390/microorganisms11030629.
10. Ahmad SA, Das SS, Khatoon A, Ansari MT, Afzal M, Hasnain MS, et al. Bactericidal activity of silver nanoparticles: a mechanistic review. Mater Sci Energy Technol. 2020;3:756–69. https://doi.org/10.1016/j.mset.2020.09.002.
11. Ong WTJ, Nyam KL. Evaluation of silver nanoparticles in cosmeceutical and potential biosafety complications. Saudi J Biol Sci. 2022;29(4):2085–94. https://doi.org/10.1016/j.sjbs.2022.01.035.
12. Bruna T, Maldonado-Bravo F, Jara P, Caro N. Silver nanoparticles and their antibacterial applications. Int J Mol Sci. 2021;22(13):7202. https://doi.org/10.3390/ijms22137202.
13. Kędziora A, Speruda M, Krzyżewska E, Rybka J, Łukowiak A, Bugla-Płoskońska G. Similarities and differences between silver ions and silver in nanoforms as

antibacterial agents. Int J Mol Sci. 2018;19(2):444. https://doi.org/10.3390/ijms19020444.

14. Nguyen NPU, Dang NT, Doan L, Nguyen TTH. Synthesis of silver nanoparticles: from conventional to ‘modern’ methods—a review. Processes. 2023;11(9):2617. https://doi.org/10.3390/pr11092617.
15. Vishwanath R, Negi B. Conventional and green methods of synthesis of silver nanoparticles and their antimicrobial properties. Curr Res Green Sustain Chem. 2021;4:100205. https://doi.org/10.1016/j.crgsc.2021.100205.
16. Xu L, Wang Y-Y, Huang J, Chen C-Y, Wang Z-X, Xie H. Silver nanoparticles: synthesis, medical applications and biosafety. Theranostics. 2020;10(20):8996–9031. https://doi.org/10.7150/thno.45413.
17. Sakamoto M, Fujistuka M, Majima T. Light as a construction tool of metal nanoparticles: synthesis and mechanism. J Photochem Photobiol C Photochem Rev. 2009;10(1):33–56. https://doi.org/10.1016/j.jphotochemrev.2008.11.002.
18. Harada M, Saijo K, Sakamoto N. Characterization of metal nanoparticles prepared by photoreduction in aqueous solutions of various surfactants using UV–vis, EXAFS and SAXS. Colloids Surf A Physicochem Eng Asp. 2009;349(1-3):176–88. https://doi.org/10.1016/j.colsurfa.2009.08.015.
19. Liu H, Ge Q, Xu F, Qu X, Fu H, Sun J. Dissolved black carbon induces fast photo-reduction of silver ions under simulated sunlight. Sci Total Environ. 2021;775:145897. https://doi.org/10.1016/j.scitotenv.2021.145897.
20. Wang T-J, Chang H-W, Chen J-S, Chiang H-P. Nanotip-assisted photoreduction of silver nanostructures on chemically patterned ferroelectric crystals for surface

enhanced Raman scattering. Sci Rep. 2019;9(1):10962. https://doi.org/10.1038/s41598-019-47523-8.

21. Liu Y-Q, Zhu W, Yuan Q, Hu J-M, Zhang X, Shen A-G. Photoreduced Ag+ surrounding single poly(4-cyanostyrene) nanoparticles for undifferentiated SERS sensing and killing of bacteria. Talanta. 2022;245:123450. https://doi.org/10.1016/j.talanta.2022.123450.
22. Shui L, Zhang G, Hu B, Chen X, Jin M, Zhou G, et al. Photocatalytic one-step synthesis of Ag nanoparticles without reducing agent and their catalytic redox performance supported on carbon. J Energy Chem. 2019;36:37–46. https://doi.org/10.1016/j.jechem.2019.04.006.
23. Silva-de-Hoyos LE, Sánchez-Mendieta V, Rico-Moctezuma A, Vilchis-Nestor AR, Camacho-López MA, Avalos-Borja M. Silver nanoparticles biosynthesized using *Opuntia ficus* aqueous extract. Superf Vacío. 2012;25(1):31–5.
24. Luu TLA, Cao XT, Nguyen VT, Pham NL, Nguyen HL, Nguyen CT. Simple controlling ecofriendly synthesis of silver nanoparticles at room temperature using lemon juice extract and commercial rice vinegar. J Nanotechnol. 2020;2020:3539701. https://doi.org/10.1155/2020/3539701.
25. Sarkandi AF, Montazer M, Harifi T, Rad MM. Innovative preparation of bacterial cellulose/silver nanocomposite hydrogels: *in situ* green synthesis, characterization, and antibacterial properties. J Appl Polym Sci. 2021;138(6):49824. https://doi.org/10.1002/app.49824.
26. Vasconcelos NF, Feitosa JPA, da Gama FMP, Morais JPS, Andrade FK, Filho MDSMDS, et al. Bacterial cellulose nanocrystals produced under different

hydrolysis conditions: properties and morphological features. Carbohydr Polym. 2017;155:425–31. https://doi.org/10.1016/j.carbpol.2016.08.090.

27. Foresti ML, Vázquez A, Boury B. Applications of bacterial cellulose as precursor of carbon and composites with metal oxide, metal sulfide and metal nanoparticles: a review of recent advances. Carbohydr Polym. 2017;157:447–67. https://doi.org/10.1016/j.carbpol.2016.09.008.

28. Valencia L, Kumar S, Nomena EM, Salazar-Alvarez G, Mathew AP. *In-situ* growth of metal oxide nanoparticles on cellulose nanofibrils for dye removal and antimicrobial applications. ACS Appl Nano Mater. 2020;3(7):7172–81. https://doi.org/10.1021/acsanm.0c01511.

29. Pal S, Nisi R, Stoppa M, Licciulli A. Silver-functionalized bacterial cellulose as antibacterial membrane for wound-healing applications. ACS Omega. 2017;2(7):3632–9. https://doi.org/10.1021/acsomega.7b00442.

30. Wu J, Zheng Y, Song W, Luan J, Wen X, Wu Z, et al. *In situ* synthesis of silver-nanoparticles/bacterial cellulose composites for slow-released antimicrobial wound dressing. Carbohydr Polym. 2014;102:762–71. https://doi.org/10.1016/j.carbpol.2013.10.093.

31. Keshk J. Bacterial cellulose production and its industrial applications. Bioprocess Biotech. 2014;4:150. https://doi.org/10.4172/2155-9821.1000150.

32. Poolman JT, Anderson AS. *Escherichia coli* and *Staphylococcus aureus*: leading bacterial pathogens of healthcare associated infections and bacteremia in older-age populations. Expert Rev Vaccines. 2018;17(7):607–18. https://doi.org/10.1080/14760584.2018.1488590.

33. Bachir G, Abouni B. *Escherichia coli* and *Staphylococcus aureus* most common source of infection. In: Méndez-Vilas A, editor. The battle against microbial pathogens: basic science, technological advances and educational programs. Spain: Formatex Research Center; 2015. p. 637–48.

34. Haindongo EH, Ndakolo D, Hedimbi M, Vainio O, Hakanen A, Vuopio J. Antimicrobial resistance prevalence of *Escherichia coli* and *Staphylococcus aureus* amongst bacteremic patients in Africa: a systematic review. J Glob Antimicrob Resist. 2023;32:35–43. https://doi.org/10.1016/j.jgar.2022.11.016.

35. Lv C, Leng J, Qian M, Sun B, Ye H, Li M, et al. Antimicrobial resistance in *Escherichia coli* and *Staphylococcus aureus* at human-animal interfaces on Chongming Island, Shanghai: a one health perspective. One Health. 2024;19:100910. https://doi.org/10.1016/j.onehlt.2024.100910.

36. Antimicrobial Resistance Collaborators. The burden of antimicrobial resistance in the Americas in 2019: a cross-country systematic analysis. Lancet Reg Health Am. 2023;25:100561. https://doi.org/10.1016/j.lana.2023.100561.

37. Morales-Cepeda AB, Díaz-Guerrero AM, Ledezma-Pérez AS, Alvarado-Canché CN, Rivera-Armenta JL. Bacterial cellulose from mother of vinegar loaded with silver nanoparticles as an effective antiseptic for wound-healing: antibacterial activity against *Staphylococcus aureus* and *Escherichia coli*. Chem Pap. 2024;78(6):3959–69. https://doi.org/10.1007/s11696-024-03366-w.

38. Abdellatif AAH, Alturki HNH, Tawfeek HM. Different cellulosic polymers for synthesizing silver nanoparticles with antioxidant and antibacterial activities. Sci Rep. 2021;11(1):84. https://doi.org/10.1038/s41598-020-79834-6.

39. Hotze EM, Phenrat T, Lowry GV. Nanoparticle aggregation: challenges to understanding transport and reactivity in the environment. J Environ Qual. 2010;39(6):1909–24. https://doi.org/10.2134/jeq2009.0462.

40. Tsuda A, Konduru NV. The role of natural processes and surface energy of inhaled engineered nanoparticles on aggregation and corona formation. NanoImpact. 2016;2:38–44. https://doi.org/10.1016/j.impact.2016.06.002.

41. Dorofte AL, Dima C, Ceoromila A, Botezatu A, Dinica R, Bleoanca I, et al. Controlled release of β-CD-encapsulated thyme essential oil from whey protein edible packaging. Coatings. 2023;13(3):508. https://doi.org/10.3390/coatings13030508.

42. Thube S, Badgujar MA. Synthesis, and characterization of several transition metal complexes derived from α-benzilmonoximethiosemicarbohydrazide and m-chlorobenzaldehyde. J Reatt Ther Dev Divers. 2023;6(10S):2166–70. https://doi.org/10.53555/jrtdd.v6i10s.2970.

43. Filopoulou A, Vlachou S, Boyatzis SC. Fatty acids and their metal salts: a review of their infrared spectra in light of their presence in cultural heritage. Molecules. 2021;26(19):6005. https://doi.org/10.3390/molecules26196005.

44. Zhang F, Huang L, Zou J, Yang J, Kang X, Chen S. Isonitrile-functionalized ruthenium nanoparticles: intraparticle charge delocalization through Ru=C=N interfacial bonds. J Nanoparticle Res. 2017;19(9):308. https://doi.org/10.1007/s11051-017-4010-8.

45. Kim Y, Park Y, Han S, Park W, Kim M, Kim K, et al. Radiative and non-radiative decay pathways in carbon nanodots toward bioimaging and photodynamic therapy. Nanomaterials. 2021;12(1):70. https://doi.org/10.3390/nano12010070.

46. León A, Reuquen P, Garín C, Segura R, Vargas P, Zapata P, et al. FTIR and Raman characterization of TiO2 nanoparticles coated with polyethylene glycol as carrier for 2-methoxyestradiol. Appl Sci. 2017;7(1):49. https://doi.org/10.3390/app7010049.

47. Orsuwan A. Effect of cellulose nanocrystals and green synthesized silver nanoparticles on mechanical properties and antimicrobial activity of banana flour/agar composite films. Heliyon. 2023;9(4):e15102. https://doi.org/10.1016/j.heliyon.2023.e15102.

48. Vasil'kov A, Butenko I, Naumkin A, Voronova A, Golub A, Buzin M, et al. Hybrid silver-containing materials based on various forms of bacterial cellulose: synthesis, structure, and biological activity. Int J Mol Sci. 2023;24(8):7667. https://doi.org/10.3390/ijms24087667.

49. Mutiara T, Sulistyo H, Fahrurrozi M, Hidayat M. Facile route of synthesis of silver nanoparticles templated bacterial cellulose, characterization, and its antibacterial application. Green Process Synth. 2022;11(1):361–72. https://doi.org/10.1515/gps-2022-0038.

50. Rac-Rumijowska O, Maliszewska I, Fiedot-Toboła M, Karbownik I, Teterycz H. Multifunctional nanocomposite cellulose fibers doped *in situ* with silver nanoparticles. Polymers. 2019;11(3):562. https://doi.org/10.3390/polym11030562.

51. Vasil'kov A, Rubina M, Naumkin A, Buzin M, Dorovatovskii P, Peters G, et al. Cellulose-based hydrogels and aerogels embedded with silver nanoparticles: preparation and characterization. Gels. 2021;7(3):82. https://doi.org/10.3390/gels7030082.

52. Teixeira SRZ, Reis EMD, Apati GP, Meier MM, Nogueira AL, Garcia MCF, et al. Biosynthesis and functionalization of bacterial cellulose membranes with cerium nitrate and silver nanoparticles. Mater Res. 2019;22(Suppl 1):e20190054. https://doi.org/10.1590/1980-5373-mr-2019-0054.

53. Chen Q-Y, Xiao S-L, Shi SQ, Cai L-P. A one-pot synthesis and characterization of antibacterial silver nanoparticle–cellulose film. Polymers. 2020;12(2):440. https://doi.org/10.3390/polym12020440.

54. Li N, Li J, Wan X, Niu Y, Gu Y, Chen G, et al. Preparation of micro-size spherical silver particles and their application in conductive silver paste. Materials. 2023;16(4):1733. https://doi.org/10.3390/ma16041733.

55. Alsharif SM, Salem SS, Abdel-Rahman MA, Fouda A, Eid AM, El-Din Hassan S, et al. Multifunctional properties of spherical silver nanoparticles fabricated by different microbial taxa. Heliyon. 2020;6(5):e03943. https://doi.org/10.1016/j.heliyon.2020.e03943.

56. Nuñez-Figueredo Y, Sánchez-Valdes S, Ramírez-Vargas E, Ramos-deValle LF, Albite-Ortega J, Rodriguez-Fernandez OS, et al. Influence of ionic liquid on graphite/silver nanoparticles dispersion and antibacterial properties against *Escherichia coli* of PP/EPDM composite coatings. J Appl Polym Sci. 2019;137(21):48714. https://doi.org/10.1002/app.48714.

57. Barud HS, Regiani T, Marques RFC, Lustri WR, Messaddeq Y, Ribeiro SJL. Antimicrobial bacterial cellulose-silver nanoparticles composite membranes. J Nanomater. 2011;2011:721631. https://doi.org/10.1155/2011/721631.

58. Anwar Y, Ul-Islam M, Ali HSHM, Ullah I, Khalil A, Kamal T. Silver impregnated bacterial cellulose-chitosan composite hydrogels for antibacterial and catalytic applications. J Mater Res Technol. 2022;18:2037–47. https://doi.org/10.1016/j.jmrt.2022.03.089.

59. Kawakami H, Yoshida K, Nishida Y, Kikuchi Y, Sato Y. Antibacterial properties of metallic elements for alloying evaluated with application of JIS Z 2801:2000. ISIJ Int. 2008;48(9):1299–304. https://doi.org/10.2355/isijinternational.48.1299.

60. Hochvaldová L, Panáček D, Válková L, Večeřová R, Kolář M, Prucek R, et al. *E. coli* and *S. aureus* resist silver nanoparticles via an identical mechanism, but through different pathways. Commun Biol. 2024;7(1):1552. https://doi.org/10.1038/s42003-024-07266-3.

61. Somda D, Bargul JL, Wesonga JM, Wachira SW. Green synthesis of *Brassica carinata* microgreen silver nanoparticles, characterization, safety assessment, and antimicrobial activities. Sci Rep. 2024;14(1):29273. https://doi.org/10.1038/s41598-024-80528-6.

62. Qais FA, Shafiq A, Khan HM, Husain FM, Khan RA, Alenazi B, et al. Antibacterial effect of silver nanoparticles synthesized using *Murraya koenigii* (L.) against multidrug-resistant pathogens. Bioinorg Chem Appl. 2019;2019:4649506. https://doi.org/10.1155/2019/4649506.

63. Vadakkan K, Hemapriya J, Ngangbam AK, Sathishkumar K, Mapranathukaran VO. Biofilm inhibition of *Staphylococcus aureus* by silver nanoparticles derived from *Hellenia speciosa* rhizome extract. Microb Pathog. 2024;196:106933. https://doi.org/10.1016/j.micpath.2024.106933.

64. Courrol DDS, Lopes CRB, Cordeiro TDS, Franzolin MR, Junior NDV, Samad RE, et al. Optical properties and antimicrobial effects of silver nanoparticles synthesized by femtosecond laser photoreduction. Opt Laser Technol. 2018;103:233–8. https://doi.org/10.1016/j.optlastec.2018.01.044.